CMS Physics Analysis Summary

Contact: cms-pag-conveners-exotica@cern.ch 2015/01/14

Search for high-mass resonances and large extra dimensions with tau-lepton pairs decaying into final states with an electron and a muon at $\sqrt{s} = 8\,\text{TeV}$

The CMS Collaboration

Abstract

A search for new physics beyond the standard model in the high-mass ditau final state with one tau decaying in the electron channel and one tau decaying in the muon channel is performed using proton-proton collisions at $\sqrt{s}$ = 8 TeV recorded by the CMS experiment at the LHC. The data correspond to an integrated luminosity of 19.7 fb^{-1}. The data are in good agreement with the standard model prediction. An upper limit at 95% CL on the product of cross section times branching fraction into tau pairs is calculated as a function of the resonance mass for the Sequential Standard Model Z' (Z'_{SSM} masses excluded up to 1300 GeV) and for the GUT-inspired E_6 model (Z'_{ψ} masses excluded up to 810 GeV). The results are further interpreted in terms of the Arkani-Hamed, Dimopolous, and Dvali (ADD) model, setting an exclusion limit on the parameter Λ_T up to 2800 GeV.

1 Introduction

The standard model (SM) of high-energy particle physics is a successful theory that can explain many experimental observations of elementary particles at a high level of precision. It is nevertheless believed not to be an ultimate theory of nature and many models beyond the SM have been proposed.

In Grand Unified Theories (GUT) [1–6], strong and electroweak interactions are merged into a single interaction, described by a higher symmetry group. In the GUT-inspired E_6 scenario the symmetry is broken down by the following pattern:

$$E_6 \rightarrow SO(10) \times U(1)_\psi \rightarrow SU(5) \times U(1)_\chi \times U(1)_\psi \rightarrow SU(3)_C \times SU(2)_L \times U(1)_Y \times U(1)_{\theta_{E_6}}, \quad (1)$$

where $U(1)_{\theta_{E_6}}$ is believed to be broken at the TeV scale [3]. It is assumed that only one linear combination remains light:

$$Z' = Z'_\chi cos_{\theta_{E_6}} + Z'_\psi sin_{\theta_{E_6}}, \quad (2)$$

with θ_{E_6} being a free parameter of the model, in the range of $-90^\circ \leq \theta_{E_6} \leq 90^\circ$. The neutral gauge boson Z'_ψ, corresponding to the case $\theta_{E_6} = 90^\circ$, is considered in this analysis.

New neutral gauge bosons are predicted in other models beyond the SM. A useful benchmark model used in many Z' searches is the Sequential Standard Model (SSM) Z', where Z'_{SSM} is a neutral spin 1 boson that has the same couplings to quarks and leptons as the SM Z boson. The SSM is not gauge-invariant [3] unless it has different couplings to exotic fermions, or occurs as an excited state of the ordinary SM Z boson in models with extra dimensions at the weak scale [1]. However, this does not diminish its usefulness as benchmark process and so the Z'_{SSM} is used to optimise the signal event selection of the analysis.

Universality of couplings is not necessary for these new gauge bosons and models exist that include generational-dependent couplings, resulting in Z' bosons which preferentially decay to fermions of the third generation [1, 7]. For this reason it is important to search for new heavy bosons in all possible decay modes.

Results of direct searches for high-mass ditau resonances have been reported by the ATLAS [8, 9] and CMS [10] collaborations. The ATLAS results are based on an event sample of 4.6 fb^{-1} recorded at $\sqrt{s}$ = 7 TeV (Z'_{SSM} excluded for masses below 1.4 TeV at 95% CL) plus 19.5 fb^{-1} at $\sqrt{s}$ = 8 TeV (Z'_{SSM} excluded for masses below 1.9 TeV at 95% CL). The CMS result is based on an event sample of 4.9 fb^{-1} recorded at $\sqrt{s}$ = 7 TeV (Z'_{SSM} excluded for masses below 1.4 TeV at 95% CL). The most stringent mass limits on Z'_{SSM} production in the decay channel of the Z' to a pair of electrons or muons amount to 2.90 TeV in case of ATLAS [11] and 2.96 TeV in case of CMS [12].

Large extra dimensions (LED) of a finite size R beyond the four-dimensional space-time have been proposed by Arkani-Hamed, Dimopolous, and Dvali (ADD) in 1998 [13] to solve the hierarchy problem of the SM. In this model the ordinary Planck scale (M_{Pl}) is related to the fundamental Planck scale (M_D) via the formula:

$$M_{Pl}^2 = M_D^{2+n} \times R^n \quad (3)$$

where n is the number of extra dimensions. From Eq. (3), for $M_D \sim$ O(1) TeV, we have $R \lesssim$ O(1) mm, if n$\geq$2. Experiments [14–18] indicate that the cases n = 1, 2 are likely ruled out. A phenomenological effect in ADD is the anomalous production of fermion-antifermion or diboson pairs with large invariant mass stemming from the coupling to virtual gravitons.

Since difermion production via virtual graviton exchange can interfere with SM production of the same final-state particles, the cross section in the presence of LED is given by [19, 20]: $\sigma_{SM+LED} = \sigma_{SM} + \sigma_{int}\eta_G + \sigma_G\eta_G^2$, where σ_{int} and σ_G denote the interference and graviton terms in addition to the SM cross section σ_{SM}. Effects of LED are parametrised via a single variable η_G or Λ_T. They are selected by $\eta_G = 1/\Lambda_T^4 = \mathcal{F}/M_S^4$, where M_S is the ultraviolet cutoff of the sum over Kaluza–Klein excitations in virtual gravition exchange ($M_S \sim M_D$ in 4+n dimensional space) and $\mathcal{F}$ is a parameter for which different definitions exist:

$$\mathcal{F} = \begin{cases} 1 & \text{in } GRW(Giudice, Rattazzi, Wells)[19] \\ \frac{2}{n-2} & \text{in } HLZ(Han, Lykken, Zhang)\ [20],\ with\ n > 2 \end{cases} \quad (4)$$

By construction, the ADD model described above is valid below the ultraviolet cutoff. The convention used throughout this analysis is to set the cutoff at $M_{max} = \Lambda_T$ (GRW).

The most stringent limits on Λ_T in the dielectron and dimuon decay channels amount to 4.20 TeV in case of ATLAS [21] and 4.15 TeV in case of CMS [22, 23]. There are no limits on Λ_T and the other parameters of the ADD model from searches with high-mass tau pairs. Such analysis is nevertheless important to verify experimentally the limits up to which we can assume that there is no preference of virtual gravitons decaying into third generation of leptons. On the other hand, in presence of extra-SM events it will be crucial to fully identify all of their properties and in particular the coupling to the different generations of leptons.

In this note we report on a search for new physics beyond the SM in the high-mass tau pairs distribution, as expected from the Z'_{SSM}, Z'_{ψ}, and ADD models, in the final state where one tau decays in the electron channel and the other tau decays in the muon channel. Despite the lower branching ratio compared to the channels where there is at least one tau that decays hadronically, this channel is characterised by a very clean signature. Both the electron and muon are easier to handle experimentally: the reconstruction and identification efficiency is higher and the fake rate lower compared to hadronically decaying taus, and their systematic uncertainties are lower. The other fully leptonic channels (ee, $\mu\mu$) have half of branching ratio compared to the $e\mu$ channel and are overwhelmed by the SM Drell-Yan production.

A data sample of proton-proton collisions recorded at $\sqrt{s}$ = 8 TeV, corresponding to an integrated luminosity of 19.7 fb^{-1}, collected with the CMS experiment at the LHC is used.

2 The CMS experiment

The central feature of the Compact Muon Solenoid (CMS) apparatus is a superconducting solenoid, of 6 m internal diameter, providing a field of 3.8 T. Within the field volume are the silicon pixel and strip tracker, the crystal electromagnetic calorimeter (ECAL) and the brass/scintillator hadron calorimeter (HCAL). The inner tracker is composed of a pixel detector and a silicon strip tracker, and measures charged-particle trajectories in the pseudorapidity range $|\eta| < 2.5$ [1]. The finely segmented ECAL consists of nearly 76 000 lead-tungstate crystals that provide coverage in pseudorapidity up to $|\eta| = 3.0$. The muon system covers the pseudorapidity region $|\eta| < 2.4$ and consists of up to four stations of gas-ionisation muon detectors installed outside the solenoid and sandwiched between the layers of the steel return yoke. A detailed description of the CMS detector can be found elsewhere [24].

[1] A right-handed coordinate system is used in CMS, with the origin at the nominal collision point, the x axis pointing to the centre of the LHC ring, the y axis pointing up (perpendicular to the LHC plane), and the z axis along the anticlockwise beam direction. Pseudorapidity η is defined as $\eta = -\ln[\tan(\theta/2)]$, where $cos\theta = p_z/p$. The azimuthal angle ϕ is the angle relative to the positive x axis measured in the $x-y$ plane.

3 Object reconstruction and identification

Muons are reconstructed using the inner tracker and muon chambers [25]. Quality requirements, based on the minimum number of hits in the silicon tracker, pixel detector, and muon chambers, are applied to suppress backgrounds from punch-through and decays in flight.

Electrons are reconstructed as superclusters in the ECAL associated with tracks in the tracking detector [26]. Requirements are imposed to distinguish prompt electrons from charged pions and electrons produced by photon conversions.

A particle-flow algorithm [27] is used to combine information from all CMS subdetectors to identify and reconstruct individual particles in the event: muons, electrons, photons, and charged and neutral hadrons. From the resulting particle list, jets and missing transverse energy ($\overrightarrow{\not{E}_T}$) are reconstructed. The jets are reconstructed using the anti-k$_T$ jet algorithm [28, 29] with a distance parameter of R = 0.5. To tag jets coming from b-quark decays, the combined secondary vertex algorithm is used. This algorithm is based on the reconstruction of secondary vertices, together with track-based lifetime information [30]. The $\overrightarrow{\not{E}_T}$ is defined as the negative vectorial sum of the $\overrightarrow{p_T}$ of all detected particles in an event.

4 Signal and background MC samples

Monte Carlo (MC) event generators are used to simulate the signal and its SM backgrounds.

The MC simulated samples for the signal are generated with PYTHIA [31] for the three models considered in this analysis and introduced in Section 1: Z'_{SSM}, Z'_{ψ}, and ADD. Separate Z'_{SSM} and Z'_{ψ} samples are generated for nine different Z' masses, ranging from 500 to 2000 GeV in 250 GeV steps. TAUOLA [32] is used to simulate tau decays for these samples. For the ADD model, independent samples are generated for 8 different values of the parameter Λ_T, ranging from 1600 to 4400 GeV in steps of 400 GeV.

The simulation of pileup is taken into account by superimposing minimum bias interactions onto the hard scattering process, matching the pileup profile in data. MC-generated events are propagated through the full GEANT-based simulation [33] of the CMS detector [24].

The most important background sources in the search for high-mass ditau resonances are as follows: background from $\mathrm{t\bar{t}}$ ($\mathrm{t} \to \mathrm{W\,b}$) events is usually characterised by one or two jets tagged as b quark jet in addition to isolated leptons originating from the leptonic decay of the $\mathrm{W}^{\pm}$ boson. Multijet events are characterised by low charged track multiplicity jets that can misidentify leptons. The SM Drell-Yan production of tau pairs represents an irreducible background. Background from diboson events ($\mathrm{W}^{\pm}\,\mathrm{W}^{\mp}$, $\mathrm{W}^{\pm}\mathrm{Z}$, ZZ) may produce pairs of isolated leptons in case both gauge bosons decay leptonically. For the W+Jets background, the most likely scenario that would generate a background contribution is related to a very clean prompt muon from W boson decay and to a jet misidentified as an electron. Both tW and $\bar{t}\mathrm{W}$ processes (referred below together as tW) are a background when the two W bosons (one of which comes from the top decay) decay leptonically in a muon and an electron respectively. The MC samples for the $\mathrm{t\bar{t}}$ and tW processes are generated with POWHEG [34], the SM Drell-Yan and W+Jets processes with MADGRAPH [35], and all the other backgrounds with PYTHIA [31]. All samples, except W+Jets and multijet ones, are interfaced to TAUOLA [32] to simulate tau decays.

5 Event selection

The selection of signal events is performed as follows: at trigger level, events are required to contain at least two leptons, one electron plus one muon, with minimum p_{T} of the leading lepton of 17 GeV and minimum p_{T} of sub-leading lepton of 8 GeV. Events are selected if the electron has a transverse energy $E_{\mathrm{T}} > 20$ GeV and pseudorapidity $|\eta| < 2.5$ and outside the transition region between the ECAL barrel and endcap parts, $1.442 < |\eta| < 1.56$, and the muon has a transverse momentum $p_{\mathrm{T}} > 20$ GeV and $|\eta| < 2.1$.

Both the electron and the muon are required to be isolated to suppress the misidentification of jets. The electron tracker isolation requires that the sum of the p_{T} of all tracks within a cone of $\Delta R < 0.3$ ($\Delta R = \sqrt{(\Delta\eta)^2 + (\Delta\phi)^2}$) around the electron candidate's track is less than 5 GeV. The electron calorimeter isolation criteria requires that the sum of the E_{T} of calorimeter energy deposits in the same cone is less than 3% of the candidate's E_{T}. The isolation variable is corrected using the measured average energy density in the event, to minimise the dependence of selection efficiency on the number of additional proton-proton interactions in the same bunch crossing [36]. The muon isolation is computed by summing the p_{T} of all charged hadrons plus the E_{T} of all photons and of all neutral hadrons reconstructed by the particle-flow algorithm [27] within a cone of radius $\Delta R < 0.4$ around the muon track direction. For charged particles, only those associated with the primary vertex[2] are considered in the isolation variable. For neutral particles, a correction is applied to account for effects of additional interactions [37] by subtracting the energy deposited in the isolation cone by charged particles not associated with the primary vertex, multiplied by a factor of 0.5. This factor corresponds approximately to the ratio of neutral to charged hadron production in the hadronisation process of pileup interactions. The muon isolation is required to be less than 12% times the p_{T} of the muon track.

Ditau pairs are constructed from by pairing electrons and muons of opposite charge that do not overlap ($\Delta R > 0.3$).

Due to the large invariant mass of the ditau pair, the electron and muon candidates are expected to be back to back. Events are therefore required to satisfy $cos\Delta\phi(\mu, e) < -0.95$, where $\Delta\phi(\mu, e)$ is the difference in the azimuthal angle among the selected candidates.

Because of the presence of neutrinos from tau decays in the signal region, the criteria $\not\!\!E_T$ >20 GeV is required. This criteria also reduces the mutijet background, whose $\not\!\!E_T$ occurs due to jet energy mismeasurements.

The direction of the missing transverse momentum is required to be consistent with originating from tau decays, to reduce the contamination of events containing $\mathrm{W}^{\pm}$ bosons. This can be achieved by introducing a variable knows as "CDF-ζ" [38], referred below as ζ variable. This variable is defined considering a unit vector along the bisector of the visible tau decay products transverse to the beam direction, denoted as the $\hat{\zeta}$ axis. Two projection variables for the visible tau decay products and $\not\!\!E_T$ are then built: $p_\zeta^{vis} = (\overrightarrow{p_T^{\mu}} + \overrightarrow{p_T^{e}}) \cdot \hat{\zeta}$ and $p_\zeta = (\overrightarrow{p_T^{\mu}} + \overrightarrow{p_T^{e}} + \overrightarrow{\not\!\!E_T}) \cdot \hat{\zeta}$. Events are selected with $p_\zeta - 3.1 \times p_\zeta^{vis} > -50$ GeV.

Residual contribution from $\mathrm{t\bar{t}}$ is minimised by selecting events with no b-tagged jets.

Moreover, an additional requirement on the difference in the azimuthal angle between the highest-p_{T} lepton (p_{T}^{ℓ}) and $\not\!\!E_{\mathrm{T}}$ is imposed, $\cos\Delta\phi(p_{\mathrm{T}}^{\ell}, \not\!\!E_{\mathrm{T}}) < 0.15$.

The signal selection efficiency after all requirements is (41 ± 1)%, (33 ± 1)%, (37 ± 1)% consid-

[2]The primary vertex is the vertex with the highest sum of the squares of the transverse momenta of tracks associated to it.

ering a Z'_{SSM} sample at mass of 1.25 TeV, a Z'_{ψ} sample at mass of 750 GeV, and a ADD sample with Λ_T of 2.4 TeV, respectively (the two taus at generator level are required to decay in the electron and the muon channels). The error quoted on the efficiency represent the statistical uncertainty from the MC samples.

To more effectively distinguish between lower mass backgrounds from tau lepton pairs from new particle production, the visible tau decay products and the $\not{E}_{\mathrm{T}}$ are used to reconstruct the mass:

$$M(\mu, e, \not{E}_T) = \sqrt{(E_\mu + E_e + \not{E}_{\mathrm{T}})^2 - (\overrightarrow{p_\mu} + \overrightarrow{p_e} + \overrightarrow{\not{E}_{\mathrm{T}}})^2}. \quad (5)$$

6 Background estimation

To estimate the background contributions in the signal region, data-driven techniques are employed wherever possible ($\mathrm{t\bar{t}}$, multijet) as described in Section 6.1. In cases where a complete data-driven approach is not possible, data-to-MC scale factors are used to correct (Drell-Yan) or to validate (WW) the expected contributions obtained from the simulated samples as explained in Section 6.2. The remaining backgrounds (WZ, ZZ, W+Jets, tW) are expected not to contribute significantly to the signal region and are estimated using the MC simulation.

6.1 Data-driven background estimations

The estimation of the background contributions in the signal region is derived from data wherever possible. The general strategy is to modify the standard selection requirements to select samples enriched with background events. These control regions are used to measure the efficiencies for background candidates to pass the signal selection requirements. Contamination from backgrounds other than the one under study in a given control region are subtracted. We perform a shape-based analysis using the mass distribution $M(\mu, e, \not{E}_T)$. The methods used to estimate the SM backgrounds into the signal region are validated using the MC simulation. We find a good agreement (compatibility below 1 standard deviation) in terms of background yield as well as in terms of the $M(\mu, e, \not{E}_T)$ shape in all closure tests.

For $\mathrm{t\bar{t}}$ background the control region is defined by selecting events with 2 b-tagged jets and applying all other event selection criteria of the signal region. The events selected in the $\mathrm{t\bar{t}}$ control region are weighted by the 0-jet to 2-jet ratio. This ratio is obtained from a second control region, defined by starting from the signal region selection but removing the 0 b-tagged jets requirement, inverting the ζ and $\cos\Delta\phi(\ell^{p_{\mathrm{T}}}, \not{E}_{\mathrm{T}})$ requirements, asking for at least one jet, and requiring $M_T(\mu, \not{E}_{\mathrm{T}}) > 90$ GeV and $M_T(e, \not{E}_{\mathrm{T}}) > 90$ GeV, with $M_T(\ell, \not{E}_{\mathrm{T}}) = \sqrt{2 \cdot p_T^l \not{E}_{\mathrm{T}}(1 - cos\Delta\phi)}$, $\ell = e, \mu$.

The multijet contribution is estimated considering like-sign ditau candidates and subtracting MC expectation of non-multijet backgrounds from data. The difference is corrected by the opposite-sign to like-sign ratio that is found to be 1.08 ± 0.04 (stat.). This ratio is measured from data in a high purity multijet region, defined with the same requirements of the signal region but inverting electron tracker and calorimeter isolation, muon isolation, and removing $\not{E}_T$ requirement.

6.2 MC-based background estimations

For the SM Drell-Yan background we compare the MC expectations with observed data in the low-mass part of the signal region ($M(\mu, e, \not{E}_T) < 200$ GeV), where no signal is expected [10]. We find a good agreement and estimate this contribution from the MC simulation applying the selection requirements of the signal region.

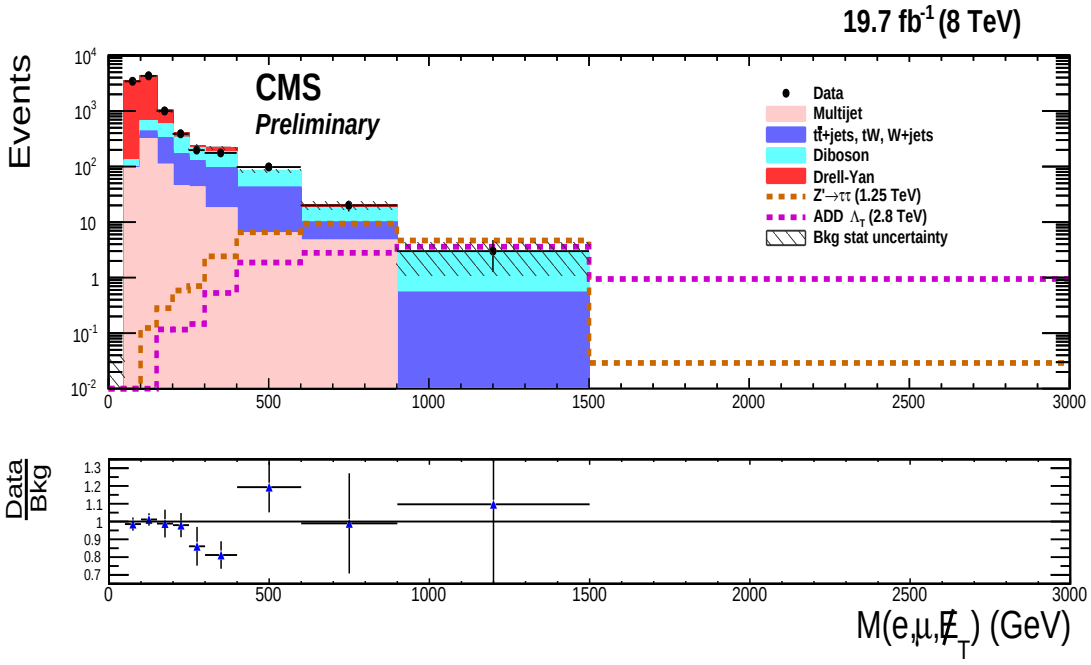

Figure 1: Distribution of the ditau mass, $M(\mu, e, \not{E}_T)$. The black points represent the observed data and the stack histogram the background expected from the SM. The lower plot shows the ratio of the data to the total SM background expectation. Error bars represent the statistical uncertainties only.

For the WW background we follow a similar approach comparing the MC expectations with observed data. The difference is that since WW is expected to be the dominant background at high mass, we do the comparison in the region of $M(\mu, e, \not{E}_T) > 200$ GeV. To reduce the signal contamination we invert the ζ cut. We introduce a lepton veto (maximum 1 muon and 1 electron with p_T >5 GeV) and jet veto (# jet = 0) to suppress other diboson backgrounds (WZ, ZZ) and $t\bar{t}$ respectively. The W+Jets contamination is reduced by tightening the electron identification variables (e.g. electron tracker isolation < 1 GeV). Using the MC information, we verify that the mass distribution in this high purity WW region preserves the same shape it has in the signal region and no bias is introduced for the comparison between data and MC expectations. We find a good agreement and estimate this contribution from the MC simulation applying the selection requirements of the signal region.

7 Results

The number of observed data and the number of background events expected from the SM are given in Table 1 for various ditau mass $M(\mu, e, \not{E}_T)$ ranges. The errors on the estimated background events represent the statistical uncertainty from the MC samples. The ditau mass $M(\mu, e, \not{E}_T)$ for the final state with an electron and a muon is shown in Fig. 1, where the black points represent the observed data and the stack histogram the background expected from the SM. Error bars are for statistical uncertainties only. As we can see, SM Drell-Yan dominates at low mass while it is negligible at high mass, where the signal would appear and $t\bar{t}$ and WW dominate instead. A good agreement between the observed data and the expected SM background is observed in the various ditau mass ranges considered.

Table 1: Number of observed events in data and estimated background events, for different $M(\mu, e, \not{E}_T)$ mass ranges. The errors on the estimated background events represent the statistical uncertainty from the MC samples.

$M(\mu, e, \not{E}_T)$ (GeV)	[50,100]	[100,150]	[150,200]	[200,250]	[250,300]
Expected bkg	3480±120	4250±130	1010±70	396±19	230±24
Data	3428	4296	1000	388	198
$M(\mu, e, \not{E}_T)$ (GeV)	[300,400]	[400,600]	[600,900]	[900,1500]	[0,1500]
Expected bkg	217±13	82±5	20±4	2.7±1.6	9680±190
Data	176	98	20	3	9607

8 Systematic uncertainties

The main source of systematic uncertainty results from the data-driven background estimation that is dominated by the statistical uncertainty on the data in the control regions. The uncertainties related to the background evaluation are taken into account through their effect on the mass shape and vary from 1% (2%) in the ditau mass bin [200,250] GeV to 55% (20%) in the ditau mass bin [900,1500] GeV for $t\bar{t}$ (multijet). The systematic uncertainty related to the lepton energy scale and resolution, as well as the variation due to jet energy scale are of order of 1% for signal and backgrounds, while we find a yield uncertainty of 3% for background and 2% for signal due to the uncertainty on the jet energy resolution. The uncertainty due to the imprecise knowledge of jet energy scale and resolution is propagated to the $\not{E}_T$. Uncertainties due to lepton isolation and identification are below 1% for background, while amounting to 2–3% for the signal. The uncertainty on the probability for a light quark or gluon jet to be misidentified as a b quark jet (10%) leads to a systematic of 0.5% for background and 1% for the signal. Imperfect modelling of pileup interaction is accounted for by introducing a systematic uncertainties of 2% for background and signal. The uncertainty on the total integrated luminosity amounts to 2.6% for 2012 data [39]. The theoretical uncertainty amounts to 6.5% for the background expectations. It includes factorisation and renormalisation scale uncertainties and the uncertainty on the parton distribution functions (PDF).

9 Interpretation of the results

No evidence of new physics decaying to a tau pair where one tau decays in the electron channel and the other tau in the muon channel is observed. We set corresponding upper limits on the existence of new neutral resonances (Z'_{SSM} and Z'_{ψ}) and on the parameters of the ADD model. We use a Bayesian method [40] for the limit extraction with a flat prior for the signal cross section and log-normal priors for the the systematic uncertainties described in Section 8. The $M(\mu, e, \not{E}_T)$ distributions from signal MC, SM backgrounds, and observed data are used as inputs in the limit computation.

The observed (solid black lines) and expected (dotted black lines) upper limits at 95% CL on the $\sigma(pp \to Z') \times \mathcal{B}(Z' \to \tau\tau)$ as a function of Z' mass and on $\sigma(pp \to G^*) \times \mathcal{B}(G^* \to \tau\tau)$ as a function of the Λ_T parameter of the ADD model are shown in Fig. 2 and Fig. 3, respectively. The coloured bands represent the one (green) and two (yellow) standard deviations obtained from the background only hypothesis.

The predicted cross section times the branching fraction to $\tau\tau$ pairs is shown where mass dependent K factors for Z' models and a K factor of 1.3 for ADD model are applied. The mass

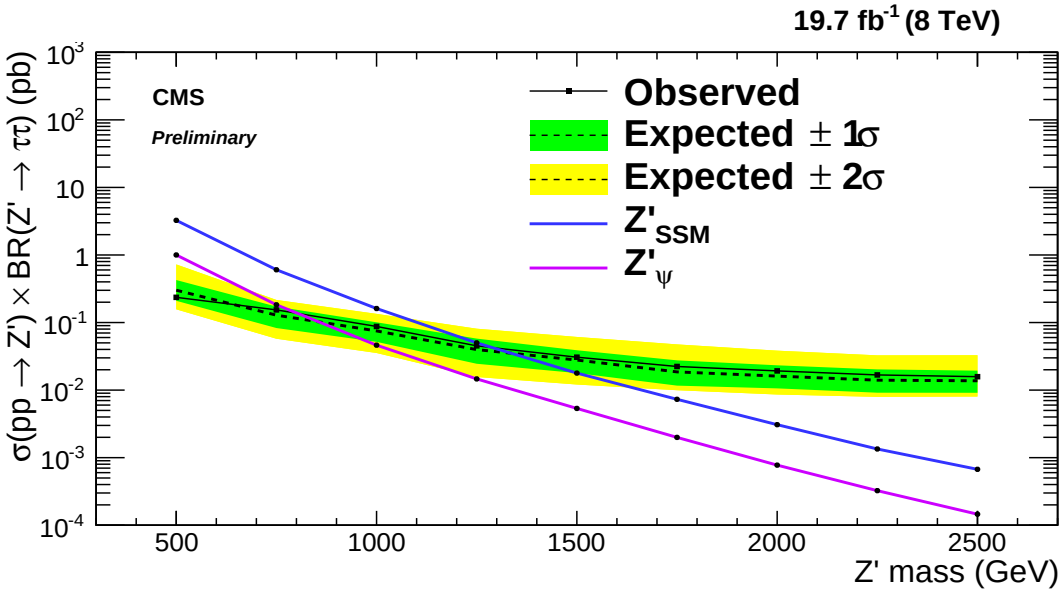

Figure 2: The observed 95% CL upper limit on $\sigma(pp \to Z') \times \mathcal{B}(Z' \to \tau\tau)$ having analysed the final state with an electron and a muon, as a function of Z' mass (solid black line). The corresponding expected limit is shown by the dotted line, and the coloured bands represent the one (green) and two (yellow) standard deviations obtained from the background only hypothesis. The Z'_{SSM} and Z'_{ψ} predicted cross section times the branching fraction to $\tau\tau$ pairs are given by the blue and violet lines. Mass dependent K factors are applied.

dependent values of the K factors are taken from the CMS searches for Z'_{SSM} and Z'_{ψ} in the ee and $\mu\mu$ decay channel [12]. The K factors are obtained using ZWPRODP [41–43] to account for the NNLO QCD contributions. The value of 1.3 is taken from the CMS searches for extra dimensions (interpretation in terms of ADD model) in the ee and $\mu\mu$ channels [22, 23]. By construction, the ADD model described above is valid below the ultraviolet cutoff. The convention used throughout this analysis is to set the cutoff at $M_{max} = \Lambda_T$ (GRW).

We exclude Z'_{SSM} with masses less than 1300 GeV and Z'_{ψ} with masses less than 810 GeV at 95% CL. Λ_T is excluded up to 2800 GeV at 95% CL. Table 2 indicates exclusion limits for the parameters of the GRW and HLZ variants introduced in Section 1.

Table 2: The observed 95% CL upper limits in terms of the parameters of the GRW and HLZ variants of the ADD model introduced in Section 1.

Limit	GRW	HLZ - M_S GeV				
	Λ_T (GeV)	n=3	n=4	n=5	n=6	n=7
Observed (K factor = 1.3)	2800	3330	2800	2530	2350	2230

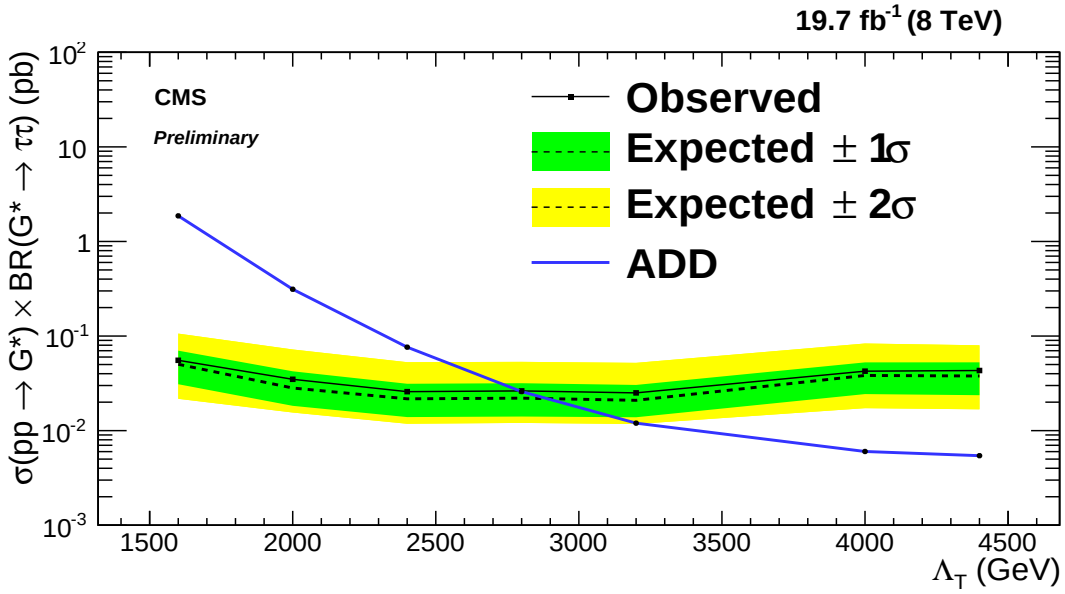

Figure 3: The observed 95% CL upper limit on $\sigma(pp \to G^*) \times \mathcal{B}(G^* \to \tau\tau)$ having analysed the final state with an electron and a muon, as a function of Λ_T parameter of the ADD model (solid black line). The corresponding expected limit is shown by the dotted line, and the coloured bands represent the one (green) and two (yellow) standard deviations obtained from the background only hypothesis. The G^* predicted cross section times the branching fraction to $\tau\tau$ pairs is given by the blue line. A K factor = 1.3 is applied.

10 Summary

A search for new physics beyond the SM with a high-mass tau lepton pair decaying to final state with an electron and a muon has been performed using proton-proton collisions at $\sqrt{s}$ = 8 TeV corresponding to an integrated luminosity of 19.7 fb^{-1}, collected by the CMS detector at the LHC. The observed mass spectrum did not reveal any evidence of new physics beyond the SM and results have been interpreted considering the Sequential Standard Model Z', the GUT-inspired E_6 model and the ADD model.

Z'_{SSM} and Z'_{ψ} have been excluded at 95% CL with masses below 1300 GeV and 810 GeV respectively. This result improves the previous limits set with 7 TeV data for the same channel of 800 and 480 GeV, while the limits from the combination of all channels at 7 TeV are 1345 and 1022 GeV [10] respectively. The Λ_T parameter of the ADD model have been excluded up to 2800 GeV.

References

[1] P. Langacker, "The Physics of Heavy Z-prime Gauge Bosons", *Rev. Mod. Phys* **81** (2009) p.1199–1228, doi:10.1103/RevModPhys81.1199, arXiv:0801.1345.

[2] A. Leike, "The Phenomenology of Extra Neutral Gauge Bosons", *Phys. Rept.* **317** (1999) 143–250, doi:10.1016/S0370-1573(98)00133-1, arXiv:hep-ph/9805494.

[3] M. Cvetic and S. Godfrey, "Discovery and Identification of Extra Gauge Bosons", *Summary of the Working Subgroup on Extra Gauge Bosons of the DPF long-range planning study published in Electro-weak Symmetry Breaking and Beyond the Standard Model, eds. T. Barklow, S. Dawson, H. Haber and J. Siegrist (World Scientific 1995), OCIP/C-95-2 UPR-648-T,* arXiv:hep-ph/9504216.

[4] T. Rizzo, "Zprime Phenomenology and the LHC", *Published in Boulder, Colliders and Neutrinos (TASI 2006), SLAC-PUB-12129,* arXiv:hep-ph/0610104.

[5] R. Diener et al., "Unravelling an Extra Neutral Gauge Boson at the LHC Using Third Generation Fermions", *Phys.Rev.D* **83** (2011) 115008, doi:10.1103/PhysRevD.83.115008, arXiv:1006.2845.

[6] J. Hewett and T. Rizzo, "Low Energy Phenomenology of Superstring Inspired E(6) Models", *Phys. Rept.* **183** (1989) p.193, doi:10.1016/0370-1573(89)90071-9.

[7] K. R. Lynch et al., "Finding Z' bosons coupled preferentially to the third family at LEP and the Tevatron", *Phys. Rev. D* **63** (2001) 035006, doi:arXiv:000728, arXiv:hep-ph/0007286.

[8] ATLAS Collaboration, "A search for high-mass resonances decaying to $\tau^+\tau^-$ in pp collisions at $\sqrt{s}$ = 7 TeV with the ATLAS detector", *Phys. Lett. B* **719** (2013) 242260, doi:10.1016/j.physletb.2013.01.040, arXiv:1210.6604.

[9] ATLAS Collaboration, "A search for high-mass ditau resonances decaying in the fully hadronic final state in pp collisions at $\sqrt{s}$ = 8 TeV with the ATLAS detector", ATLAS Notes ATLAS-CONF-2013-066, 2013.

[10] CMS Collaboration, "Search for high mass resonances decaying into τ-lepton pairs in pp collisions at $\sqrt{s}$ = 7 TeV with the CMS detector", *Phys. Lett. B* **716** (2012) 82–102, doi:10.1016/j.physletb.2012.07.062, arXiv:1206.1725.

[11] ATLAS Collaboration, "Search for high-mass dilepton resonances in pp collisions at $\sqrt{s}$ = 8 TeV with the ATLAS detector", *Submitted to Phys. Rev. D*, CERN–PH–EP–2014–053, arXiv:1405.4123.

[12] CMS Collaboration, "Search for Resonances in the Dilepton Mass Distribution in pp Collisions at $\sqrt{s}$ = 8 TeV", CMS Physics Analysis Summary CMS-PAS-EXO-12-061, 2013.

[13] N. Arkani-Hamed, S. Dimipoulos, and G. Dvali, "The hierarchy problem and new dimensions at a millimeter", *Phys. Lett. B* **429** (1998) 263–272, doi:10.1016/S0370-2693(98)00466-3, arXiv:hep-ph/9803315.

[14] G. Landsberg, "Extra Dimensions and More. . . .", Proceeding - 36th Rencontre de Moriond 2001, QCD and high Energy Hadronic Interactions.

[15] C. Hoyle et al., "Submillimeter Test of the Gravitational Inverse-Square Law: A Search for Large Extra Dimensions", *Phys. Rev. D* **86** (2001) 1418, doi:10.1103/PhysRevD.70.042004, arXiv:hep-ph/0405262.

[16] S. Cullen and M. Perelstein, "SN1987A Constraints on Large Compact Dimensions", *Phys.Rev.Lett.* **83** (1999) 268–271, doi:10.1103/PhysRevLett.83.268, arXiv:hep-ph/9903422.

[17] L. Hall and D. Smith, "Cosmological constraints on theories with large extra dimensions", *Phys. Rev. D* **60** (1999) 085008, doi:10.1103/PhysRevD.60.085008, arXiv:hep-ph/990426.

[18] C. Hanhart et al., "Extra dimensions, SN1987a, and nucleon-nucleon scattering data", *Nucl.Phys* **B595** (2001) 335–359, doi:10.1016/S0550-3213(00)00667-2, arXiv:nucl-th/0007016.

[19] G. Giudice, R. Rattazzi, and J. Wells, "Quantum Gravity and Extra Dimensions at High-Energy Colliders", *Nucl. Phys. B* **544** (1999) 338, doi:10.1016/S0550-3213(99)00044-9, arXiv:hep-ph/9811291.

[20] T. Han, J.D. Lykken, and R.J. Zhang, "On Kaluza-Klein States from Large Extra Dimensions", *Phys. Rev. D* **59** (1999) 105006, doi:10.1103/PhysRevD.59.105006, arXiv:hep-ph/9811350.

[21] ATLAS Collaboration, "Search for contact interactions and large extra dimensions in the dilepton channel using proton-proton collisions at $\sqrt{s}$ = 8 TeV with the ATLAS detector", *Submitted to Eur. Phys. J. C*, arXiv:1407.2410.

[22] CMS Collaboration, "Search for Large Extra Dimensions in Dimuon Events in pp Collisions at $\sqrt{s}$ = 8 TeV", CMS Physics Analysis Summary CMS-PAS-EXO-12-027, 2013.

[23] CMS Collaboration, "Search for Large Extra Spatial Dimensions in Dielectron Production with the CMS Detector", CMS Physics Analysis Summary CMS-PAS-EXO-12-031, 2013.

[24] CMS Collaboration, "The CMS experiment at the CERN LHC", *JINST* **3** (2008) S08004, doi:10.1088/1748-0221/3/08/S08004.

[25] CMS Collaboration, "Performance of muon identification in pp collisions at $\sqrt{s}$ = 7 TeV", CMS Physics Analysis Summary CMS-PAS-MUO-10-002, 2010.

[26] CMS Collaboration, "Electron reconstruction and identification at $\sqrt{s}$ = 7 TeV", CMS Physics Analysis Summary CMS-PAS-EGM-10-004, 2010.

[27] CMS Collaboration, "Particle-Flow Event Reconstruction in CMS and Performance for Jets, Taus, and MET", CMS Physics Analysis Summary CMS-PAS-PFT-09-001, 2009.

[28] M. Cacciari, G. P. Salam, and G. Soyez, "FastJet user manual", CERN–PH–TH (2011) 297, arXiv:1111.6097.

[29] M. Cacciari and G. P. Salam, "Dispelling the N^3 myth for the k_t jet-finder", *Phys. Lett. B* **641** (2006) 57–61, doi:10.1016/j.physletb.2006.08.037, arXiv:hep-ph/0512210.

[30] CMS Collaboration, "Identification of b-quark jets with the CMS experiment", *JINST* **8** (2013) P04013, doi:10.1088/1748-0221/8/04/P04013, arXiv:1211.4462.

[31] T. Sjostrand, S. Mrenna, and P. Skands, "PYTHIA 6.4 Physics and Manual", *JHEP* **05** (2006) 026, doi:10.1088/1126-6708/2006/05/026, arXiv:hep-ph/0603175.

[32] Z. Was et al., "TAUOLA the library for tau lepton decay", *Nucl.Phys.Proc.Suppl.* **98** (2001) 96–102, doi:10.1016/S0920-5632(01)01200-2, arXiv:hep-ph/0011305.

[33] GEANT4 Collaboration, "Geant4-a simulation toolkit", *Nucl. Instrum. Meth. A* **506** (2003) 250, doi:doi:10.1016/S0168-9002(03)01368-8.

[34] S. Frixione, P. Nason and C. Oleari, "Matching NLO QCD computations with Parton Showersimulations: the POWHEG method", *JHEP* **11** (2007) 070, doi:10.1088/1126-6708/2007/11/070, arXiv:0709.2092.

[35] J. Alwall et al., "MadGraph 5 : Going Beyond", *JHEP* **1106** (2011) 128, doi:10.1007/JHEP06(2011)128, arXiv:1106.0522.

[36] M. Cacciari and G. P. Salam, "Pileup subtraction using jet areas", *Phys. Lett. B* **659** (2008) 119–126, doi:doi:10.1016/j.physletb.2007.09.077, arXiv:0707.1378.

[37] CMS Collaboration, "Search for neutral Higgs bosons decaying to tau pairs in pp collisions at $\sqrt{s}$ = 7 TeV", *Physics Letters B* **713** (2012) 68–90, doi:10.1016/j.physletb.2012.05.028, arXiv:1202.4083.

[38] CDF Collaboration, "Search for neutral MSSM Higgs bosons decaying to tau pairs in p-pbar collisions at $\sqrt{s}$=1.96 TeV", *Phys. Rev. Lett.* **96** (2006) 011802, doi:10.1103/PhysRevLett.96.011802, arXiv:hep-ex/0508051.

[39] CMS Collaboration, "CMS Luminosity Based on Pixel Cluster Counting - Summer 2013 Update", CMS Physics Analysis Summary CMS-PAS-LUM-13-001, 2013.

[40] G. Cowan, "PDG Review on statistics (chap. 33)", *JPG* **37** (2010) 07502.

[41] E. Accomando et al., "Z' physics with early LHC data", *Phys. Rev. D* **83** (2011) 075012, doi:10.1103/PhysRevD.83.075012, arXiv:1010.6058.

[42] R. Hamberg, W. L. van Neerven, and T. Matsuura, "A complete calculation of the order α_S^2 correction to the DrellYan K-factor", *Nucl.Phys. B* **359** (1991) 343–405, doi:10.1016/0550-3213(91)90064-5.

[43] W. L. van Neerven and E. B. Zijlstra, "The O(α_S^2) corrected DrellYan K-factor in the DIS and $\bar{M}S$ schemes", *Nucl. Phys. B* **382** (1992) 11–62, doi:10.1016/0550-3213(92)90078-P.